Theoretical study of isolated dangling bonds, dangling bond wires, and dangling bond clusters on a H:Si(001)-(2×1) surface

Hassan Raza
NSF Network for Computational Nanotechnology and School of Electrical and Computer Engineering, Purdue University, West Lafayette, Indiana 47907, USA

(Received 30 November 2006; revised manuscript received 14 March 2007; published 9 July 2007)

We theoretically study the electronic band structure of isolated unpaired and paired dangling bonds (DBs), DB wires, and DB clusters on H:Si(001)-(2×1) surface using extended Hückel theory and report their effect on the Si band gap. We show that an isolated unpaired DB introduces a near-midgap state, whereas a paired DB leads to π and π^* states, similar to those introduced by an unpassivated asymmetric dimer (AD) Si(001)-(2×1) surface. On the other hand, the surface state induced due to an unpaired DB wire in the direction along the dimer row (referred to as $[\bar{1}10]$) has a large dispersion due to the strong coupling between the adjacent DBs, being 3.84 Å apart. However, in the direction perpendicular to the dimer row (referred to as [110]), the DBs are 7.68 Å apart and there is a reduced coupling between them due to exponential dependence of the wave function, leading to a small dispersion. Moreover, a paired DB wire in the $[\bar{1}10]$ direction introduces π and π^* states similar to those of an AD surface, but with a large dispersion, and a paired DB wire in the [110] direction exhibits surface states with a smaller dispersion, as expected. Besides this, we report the electronic structure of different DB clusters, which exhibit states inside the band gap that can be interpreted as superpositions of states due to unpaired and paired DBs.

DOI: 10.1103/PhysRevB.76.045308 PACS number(s): 73.20.−r, 73.20.At

I. INTRODUCTION

Due to their importance in Si technology, states induced by the dangling bonds (DBs) on Si(001) surface, known as P_b centers, have been a topic of study for decades.[1–14] These states are important due to being inside the band gap,[1,4,10–12,14] Fermi level pinning,[15] charging issue (consider variation of threshold voltage due to charged DBs), reliability issues (consider negative bias temperature instability),[16] and enhancement of gate leakage $1/f$ noise.[17] With advances in nanoscale science, a detailed understanding of these surface states is needed to exploit their role in possible technological applications, e.g., use of DB as a template for the growth of molecular nanostructures.[18] This realization has been the motivation behind research such as desorption of H from Si surface forming a DB,[19–21] electronic and electrostatic effect of DB on transport through a styrene wire,[14,22] DB dynamics on Si surface,[23] Jahn-Teller distortion in DB wires at low temperature,[24] magnetism in DB structures,[25–27] passivation of DBs with H and D,[28] scanning tunneling spectroscopy of DB wires[11] and DB clusters,[29] etc.

Watanabe *et al.*[10] predicted that an unpaired DB (Si dimer with one hydrogenated atom) wire on H:Si(001)-(2×1) surface in the direction along the dimer row would introduce states inside the band gap. This prediction was later experimentally observed; however, the mechanism is still not clear.[11] Recently, Cakmak and Srivastava[30] reproduced their results theoretically and found a similar trend. All these calculations were based on the density-functional theory where the band gap is underestimated.[31] It is thus hard to benchmark the results quantitatively. In this paper, we use extended Hückel theory (EHT) for electronic band-structure calculations using transferable parameters developed by Cerda and Soria.[32] Notably, EHT gives correct Si bulk band gap and other features as reported by Kienle *et al.*[33] It has been applied to Si surfaces obtaining satisfactory results.[33,34] The state of the art in electronic structure calculations for Si is the GW approximation.[35,36] However, computational complexity prohibits its use in transport calculations for large systems like the ones discussed in this paper where the Si atoms per unit cell may approach about 800. EHT provides computationally accessible, yet accurate approach and is worth pursuing because it overcomes some of the shortcomings of the more sophisticated methods. To the best of our knowledge, there has not yet been a systematic study of isolated DBs, DB wires, and DB clusters on H:Si(001)-(2×1) surface using a method that quantitatively addresses

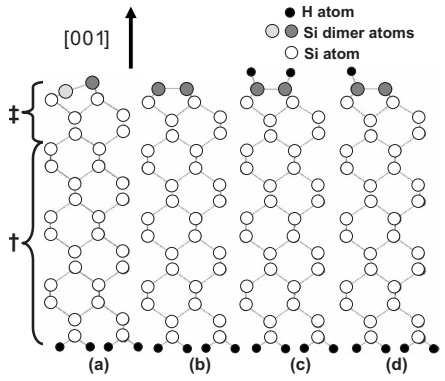

FIG. 1. Ball and stick model of 16 layer Si(001)-(2×1) unit cell used to construct different surfaces. The top four layers, represented by ‡, are relaxed due to surface reconstruction. The bottom 12 layers, represented by †, are bulk layers. (a) Unpassivated asymmetric dimer (AD) unit cell referred to as paired dangling bond (DB) configuration. (b) Unpassivated symmetric dimer (SD) unit cell. (c) Hydrogenated SD unit cell. (d) Hydrogenated unit cell with one DB referred to as unpaired DB. The back surface is hydrogenated to eliminate any DB-induced states.

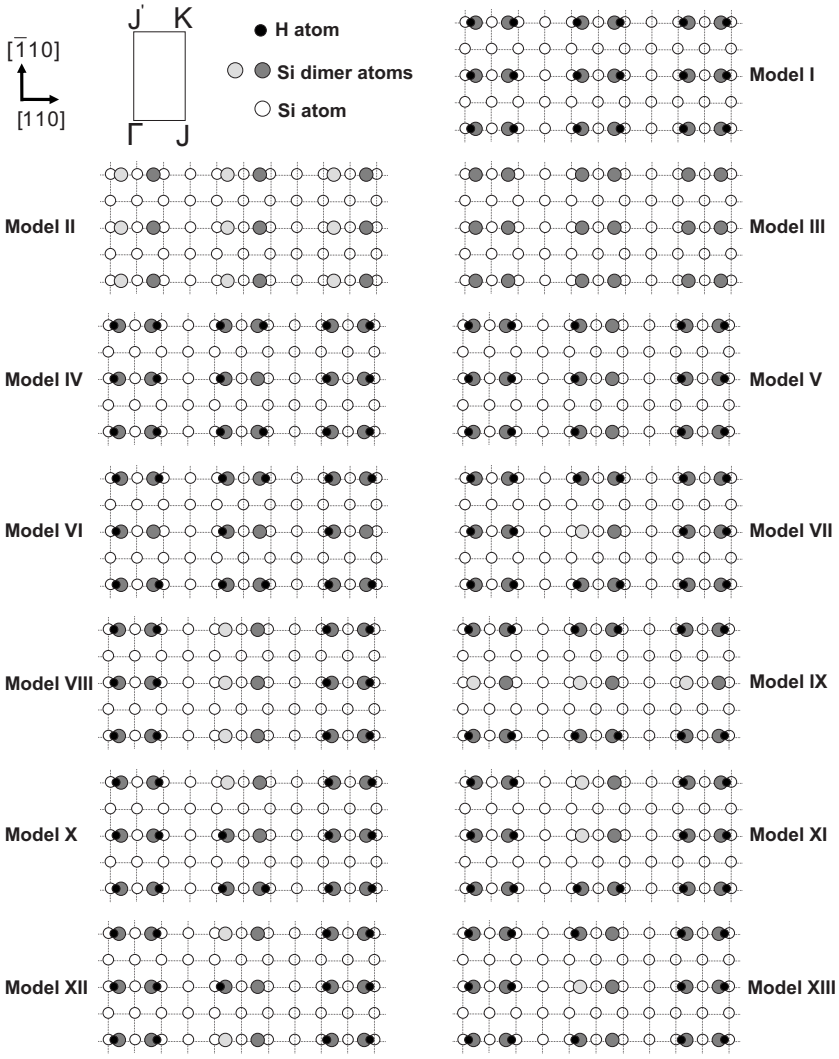

FIG. 2. Ball and stick model for the different surfaces used to calculate the electronic structure. The model numbers are the same as in Table I. A portion of the surface Brillouin zone, with different symmetry points (Γ, J, K, J'), is shown.

the surface states. Motivated by this, we study these different DB configurations on Si surface using EHT and compare the results with previously reported theory and experiments.

Apart from the scientific curiosity, these surface states may be important in practical applications, e.g., in the context of dangling bond regulated transport through a styrene chain.[14] Furthermore, these states may lead to multiple negative differential resistance (NDR) events when a molecular level is driven past these states due to applied bias, as compared to a single NDR event when a molecular level crosses the band edge, which was predicted by Rakshit *et al.*[37] Apart from this, in the field of metal based molecular electronics, there has been this notion of metal-induced states in the highest occupied molecular orbital-lowest unoccupied molecular orbital (HOMO-LUMO) gap. In Si based molecular electronics, one can analogously anticipate DB-induced states in the HOMO-LUMO gap, when the molecule being probed is in the vicinity of such DBs.

In a previous study,[14] we report that a DB electronically affects Si atoms up to about 10 Å away from it by introducing a near-midgap state in the local density of states of the neighboring Si atoms. The dispersion in the electronic structure reported in this paper is related to this length scale. Therefore, to simulate DBs in isolated, wired, and clustered configurations, we use a large enough unit cell to avoid inadvertent interaction amongst DBs in different unit cells. Figure 1 shows the unit cells being used to construct bigger unit cells corresponding to different surfaces as shown in Fig. 2 and summarized in Table I. The calculated electronic structure properties are shown in Figs. 3–5.

This paper is divided into four sections. In Sec. II, we discuss the atomic structure of different surfaces used and the corresponding assumptions made. In Sec. III, we briefly discuss the theoretical approach. In Sec. IV, we discuss the results and provide their interpretation in relevance with the past theoretical and experimental work. Finally in Sec. V, we provide the conclusions.

II. ATOMIC STRUCTURE AND ASSUMPTIONS

We use atomic structure of reconstructed Si(001)-(2×1) surface as reported by Ramstad *et al.*[38] where the top four layers are relaxed due to surface reconstruction. Ramstad *et al.*[38] report the structure for five layers of Si(001)-(2×1) asymmetric dimer (AD) surface and Si(001)-(2×1) symmetric dimer (SD) surface. We add 11 bulk layers to make a 16 layer structure and finally passivate the bottom layer with H in dihydride configuration as shown in Figs. 1(a) and 1(b),

TABLE I. Details of the unit cells used to simulate different surfaces. Sixteen layer atomic structures shown in Fig. 1 are used to construct bigger unit cells. Thus, an (8×8) unit cell has four repeating unit cells (shown in Fig. 1) in the [110] direction (perpendicular to dimer row) and eight unit cells (shown in Fig. 1) in the $[\bar{1}10]$ direction (along dimer row). The dimensions of the unit cells for isolated DB, DB wire, and DB cluster are adopted in such a way that the DB in one unit cell does not interfere with the neighboring unit cells in any inadvertent way. The total number of Si atoms (excluding H atoms on top and back surfaces) per unit cell is given.

Model	Unit-cell surface	Unit cell[a]	Atoms[b]
I	H:Si(001)-(2×1)	2×1	32
II	Si(001)-(2×1)-AD	2×1	32
III	Si(001)-(2×1)-SD	2×1	32
IV	Unpaired DB	6×6	576
V	Unpaired DB wire[c]	6×1	96
VI	Unpaired DB wire[d]	2×6	192
VII	Paired DB	6×6	576
VIII	Paired DB wire[c]	6×1	96
IX	Paired DB wire[d]	2×6	192
X	Unpaired and paired DBs[c]	6×7	672
XI	Two paired DBs[d]	6×7	672
XII	Paired, unpaired, and paired DBs[c]	6×8	768
XIII	Unpaired, paired, and unpaired DBs[c]	6×8	768

[a]Multiples of 3.84 Å (lattice constant of bulk unit cell).
[b]Number of Si atoms only per unit cell.
[c]In the $[\bar{1}10]$ direction.
[d]In the [110] direction.

respectively. We then add H atoms to each of the Si dimer atoms of Si(001)-(2×1)-SD structure, resulting in H:Si(001)-(2×1) structure as shown in Fig. 1(c). Furthermore, we remove one of the H atoms from H:Si(001)-(2×1) so that the resulting structure has an unpaired DB as shown in Fig. 1(d). The H atoms that are added have H–Si bond length=1.47 Å and H-Si dimer angle=111°. The bond length and the angle are obtained after structural optimization of a Si_9H_{14} cluster using local spin density approximation with 6-311g* basis set [calculations are performed using GAUSSIAN (Ref. 39)]. The atomic coordinates for Si(001)-(2×1)-AD unit cell [see Fig. 1(a)] and H:Si(001)-(2×1) unit cell [see Fig. 1(c)] are given here.[40,41] We use 16 layers of the unit cells to avoid any quantum confinement effects, which is further discussed in Sec. IV.

These four unit cells, shown in Figs. 1(a)–1(d), are used as building blocks to construct the bigger unit cells for doing isolated DB, DB wire, and DB cluster calculations. In the $[\bar{1}10]$ and [110] directions, along and perpendicular to the dimer rows, respectively, the unit cell consists of varying layers of Si atoms depending on the requirement. For example, to study an isolated unpaired DB, we need to include enough H:Si layers in the $[\bar{1}10]$ and [110] directions so that the DBs in adjacent unit cells do not influence each other. It should be noted that since DBs affect the neighboring Si atoms within 10 Å, two DBs would be isolated if they are at least 20 Å apart. This information is obtained from our previous study,[14] that a DB affects neighboring atoms up to approximately 10 Å. Thus, by using a (6×6) unit cell for an isolated DB, it is made sure that DBs in consecutive unit cells are electronically isolated. The calculated electronic structure is thus that of an isolated DB. Similarly, DB wires and DB clusters are also spaced sufficiently apart. Table I summarizes the dimensions of the unit cells and the number of atoms used to simulate different surfaces labeled as I–XIII. Figure 2 shows corresponding surfaces with the labels, which are used for calculating electronic band structure of isolated DBs, DB wires, and DB clusters. Figure 2 also shows part of the surface Brillouin zone used in the calculation [with symmetry points (Γ,J,K,J') (Ref. 31)]. The atoms are color coded to match Fig. 1.

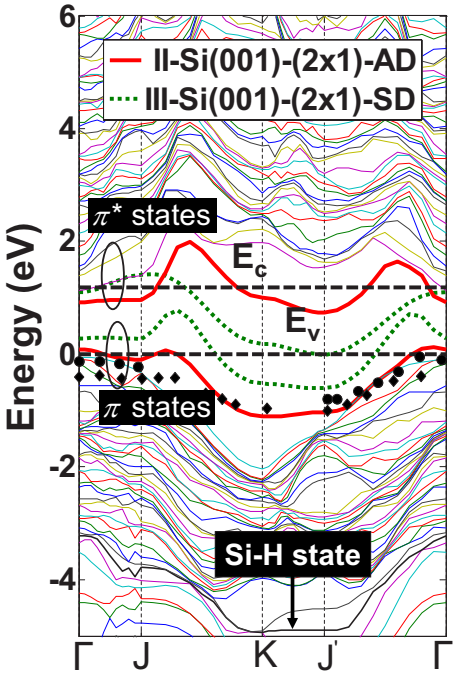

FIG. 3. (Color online) Calculated electronic band structure of H:Si(001)-(2×1), Si(001)-(2×1)-AD, and Si(001)-(2×1)-SD surfaces. The band structure of H:Si(001)-(2×1) surface shows a clean band gap. All the states are shown for this surface with various colors. The Si-H bonding state band is shown as well, having a dispersion of about 1 eV due to strong hybridization with the valence-band states. This Si-H state does not appear in the unpassivated surfaces. For Si(001)-(2×1)-AD and -SD surfaces, only π and π^* states are shown. Similarly, π and π^* states of Si(001)-(2×1)-SD surface spread throughout the band gap. H:Si(001)-(2×1) surface has a clean band gap. Si(001)-(2×1)-AD surface has 0.6 eV and Si(001)-(2×1)-SD surface has no band gap due to the π and π^* states. The diamonds and circles are experimental data points from Refs. 44 and 45, respectively.

For H:Si(001)-(2×1), Cakmak and Srivastava[30] report that the Si–Si bond length within the dimer is 2.35 Å as compared to 2.23 Å for Si(001)-(2×1)-SD as obtained by Ramstad *et al.*,[38] suggesting an increase of approximately 5% in the Si dimer distance. The surface states after passivation are, however, well below the valence-band edge (E_v) and thus do not affect the band gap. It has also been reported

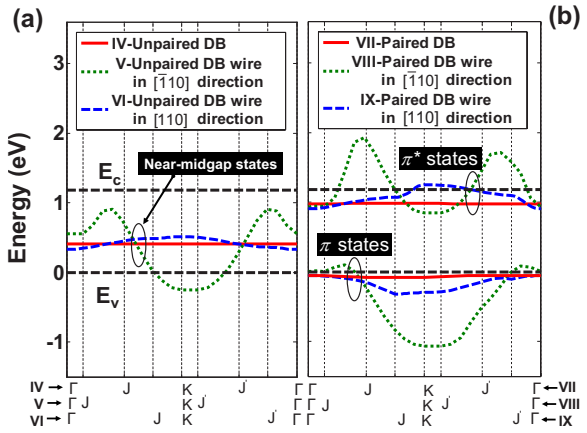

FIG. 4. (Color online) Calculated electronic band structure of periodic unit cells containing isolated DBs and DB wires. (a) Band structure of periodic unit cells containing an unpaired DB and an unpaired DB wire in the $[\bar{1}10]$ and $[110]$ directions. The unpaired DB introduces a near-midgap state whose dispersion is small. The surface states due to an unpaired DB wire in the $[\bar{1}10]$ direction have a large dispersion due to DBs being 3.84 Å apart. For the unpaired DB wire in the $[110]$ direction, DBs being farther apart (7.68 Å), the states are less dispersed. (b) Electronic band structure of periodic unit cells containing a paired DB and a paired DB wire in the $[\bar{1}10]$ and $[110]$ directions. The paired DB introduces π and π^* states very similar to the ones introduced by Si(001)-(2 $\times$1)-AD surface; however, the dispersion is much smaller. The DBs in the paired DB wire in $[\bar{1}10]$ are only 3.84 Å apart and interact in a fashion similar to AD surface, leading to considerable dispersion of the DB states. Similarly, for the paired DB wire in the $[110]$ direction, because the DBs are now farther apart, the surface states appear more like those of an isolated DB pair. The symmetry points (Γ, J, K, J') along surface Brillouin zone for different models are shown according to scale.

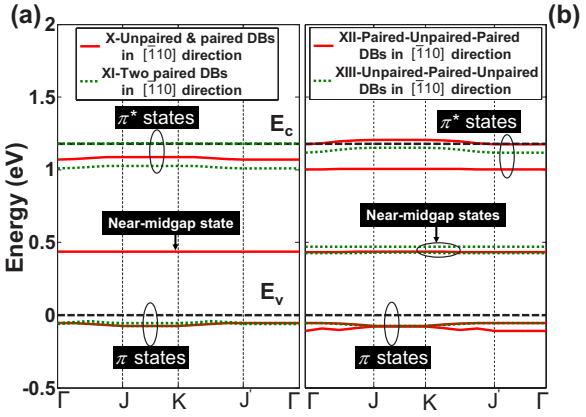

FIG. 5. (Color online) Calculated electronic band structure of periodic unit cells containing different DB clusters. (a) Cluster of an unpaired and a paired DB in the $[\bar{1}10]$ direction and of two paired DBs in the $[\bar{1}10]$ direction. (b) Cluster of paired-unpaired-paired DBs in the $[\bar{1}10]$ direction and of unpaired-paired-unpaired DBs in the $[\bar{1}10]$ direction.

elsewhere[10,30] that an unpaired DB introduces a structural perturbation in H:Si(001)-(2$\times$1) structure, which is weak. We find that using this structure for Si dimer, the surface state is shifted by approximately 20 meV (not shown here). At room temperature, this surface relaxation is anticipated to have a small effect and, hence for simplicity, we ignore it in our calculations. Furthermore, DB wires can go through Peierls distortion.[10] It has, however, been reported[10] that the total energy gain due to such distortion is 14 meV and is not anticipated to have a large effect at room temperature. Moreover, Jahn-Teller distortion in DB clusters at low temperature has been discussed in Ref. 24. The effects due to these structural changes are anticipated to be small at room temperature and hence ignored in our study. Apart from this, the effects of dopant atoms and other defects (both surface and bulk) are also ignored in our calculations. Notably, these effects have recently been examined theoretically in Ref. 42. All the atomic visualizations in this paper are done using GAUSSVIEW.[43]

III. THEORETICAL APPROACH

We model the Si surface by using a periodic system of unit cells repeating in the $[\bar{1}10]$ and $[110]$ directions. The lattice is defined by $p\vec{A}_1+q\vec{A}_2$, where $\vec{A}_1$ and $\vec{A}_2$ are lattice unit vectors in the $[\bar{1}10]$ and $[110]$ directions, p and q are indexes representing the repeating unit cells in $\vec{A}_1$ and $\vec{A}_2$ directions, respectively. The number of neighboring unit cells depends on the size of the unit cell used to represent a particular surface. Hamiltonian (H) and overlap (S) matrices are computed in EHT scheme using parameters developed by Cerda and Soria.[32] With periodic boundary conditions in the $[\bar{1}10]$ and $[110]$ directions, Fourier transform technique is used to transform H and S from the real space to the reciprocal (k) space following the scheme as follows:

$$H(\vec{k}) = \sum_{m=1}^{N} H_{mn} e^{i\vec{k}\cdot(\vec{d}_m - \vec{d}_n)}, \quad (1)$$

$$S(\vec{k}) = \sum_{m=1}^{N} S_{mn} e^{i\vec{k}\cdot(\vec{d}_m - \vec{d}_n)}, \quad (2)$$

where $\vec{k}=\vec{k}_1+\vec{k}_2$, $\vec{k}_1$ and $\vec{k}_2$ are reciprocal-lattice vectors of the surface Brillouin zone in the $[\bar{1}10]$ and $[110]$ directions, n represents the center unit cell, m represents the neighboring unit cells, N is the total number of unit cells, and $\vec{d}_m-\vec{d}_n$ is the displacement between neighboring (mth) and center (nth) unit cell. We then calculate energy eigenvalues for different values of k along the surface Brillouin-zone symmetry points (Γ, J, K, J').

IV. DISCUSSION OF RESULTS

Figure 3(a) shows the electronic band diagram of H:Si(001)-(2$\times$1) surface (model I) showing the surface and the bulk states resulting in a clean band gap of 1.18 eV. By using 16 layers in the unit cell for constructing the surface, it is made sure that the quantum confinement effects due to finite dimension of the unit cell in the [001] direction are not

present and hence do not affect the physical results as compared to the previously reported calculations (see, e.g., Refs. 10, 30, 33, and 34). Figure 3 is thus a reproduction of the work in Refs. 33 and 34, but with a larger unit cell to eliminate any quantum confinement effects. For a Si(001)-(2×1)-AD surface (model II), the π and π^* states for Si(001)-(2×1)-AD surface are shown in Fig. 3(a). The bandwidth of these states is 1.22 and 1.26 eV, respectively, due to strong electronic interaction between the paired DBs. In this case, each paired DB gets affected by the surrounding paired DBs, the most important being the two paired DBs 3.84 Å away in the $[\bar{1}10]$ direction. The band gap obtained is 0.62 eV. The dispersion properties of the π state are compared with the experimental angle-resolved photoemission spectroscopy (ARPES) observations.[44,45] The calculation and theory are consistent with each other. However, there are still some deviations on the order of few tenths of an eV, in particular, between *J* and *K* regions, but these discrepancies are within the experimental error of ARPES measurements, which is on the order of 0.1 eV. The surface states calculated using EHT match rather well with the experimental data points. The calculations done within the GW approximation[36] also agree with the experiments;[44,45] however, in the *J*-*K* range, they disagree more than the EHT calculations reported here. Similarly, for Si(001)-(2 $\times1$)-SD surface (model III), the π and π^* states disperse through the whole band gap with bandwidths of 1.39 and 1.42 eV, respectively, resulting in zero band gap. Moreover, we show the Si-H bonding state, which has a bandwidth of about 1 eV indicating a strong hybridization with the valence-band states.

Figure 4(a) shows the calculations for an isolated unpaired DB and unpaired DB wire in the $[\bar{1}10]$ and [110] directions. An isolated unpaired DB (Model IV) introduces a near-midgap state[14] (about 0.42 eV above E_v). Since this state is energetically isolated from the conduction- and the valence-band states, it does not get dispersed as shown in Fig. 4(a). For the Si/SiO_2 interface, the unpaired DB, commonly known as P_b center, has been a topic of study for decades due to its importance in the metal-oxide-semiconductor device performance and reliability. Although the chemical nature of the P_b center on Si/SiO_2 interface and unpaired DB on H:Si surface is the same, there is a significant difference due to the presence of oxygen and additional Si atoms in the case of P_b center. This difference in the environment distinguishes the two cases. However, it is worth mentioning that the P_b centers are known to introduce midgap states (for a discussion see, for example, Ref. 46). Moreover, for the unpaired DB wire in the $[\bar{1}10]$ direction (model V), the bandwidth of the near-midgap state is 1.15 eV, resulting in a very small band gap as shown in Fig. 4(a). We interpret this large dispersion to be due to the increased interaction between the DBs as being in the close proximity of 3.84 Å. Thus, each unpaired DB interacts with about four other DBs—two being 3.84 Å away and the other two being 7.68 Å away. For the unpaired DB wire in the [110] direction (model VI), since the DBs are farther apart, the coupling is reduced, resulting in a small bandwidth of 0.18 eV. This bandwidth is much smaller than that of a wire in the $[\bar{1}10]$ direction due to the exponential dependence of the wave function on distance between the DBs (to be further discussed in the next paragraph).

Figure 4(b) presents calculation for an isolated paired DB and paired DB wire in the $[\bar{1}10]$ and [110] directions. The electronic structure of a paired DB (model VII) is significantly different from an isolated unpaired DB. It introduces a bonding (π) 80 meV below E_v and antibonding (π^*) state 0.2 eV below the conduction-band edge (E_c), respectively. Qualitatively, this behavior is similar to unpassivated reconstructed Si surface. However, these states are dispersionless because the paired DBs in repeating unit cells are electronically isolated. We compare these results with the scanning tunneling spectroscopic studies of clusters of paired DBs that we will discuss later. The electronic band structure for a paired DB wire in the $[\bar{1}10]$ direction (model VIII) shows similar π and π^* states with bandwidths of about 1.23 and 1.08 eV, respectively. This large dispersion is due to strong coupling between the DBs. In this wire, each paired DB interacts with four other paired DBs—two being only 3.84 Å apart and the other two being 7.68 Å apart. As expected, the dispersion of π and π^* states for DB pair wire in the [110] direction (model IX) is less than that of the $[\bar{1}10]$ direction. The bandwidth is 0.27 and 0.35 eV for these π and π^* states, respectively, because the paired DBs are now about 5.46 Å apart. This explains higher dispersion in these states as compared to unpaired DB wire in the same direction.

In Figs. 4(a) and 4(b), only the states inside or close to the band gap are shown. Since the dimensions of the unit cell for configurations IV–IX are different, the symmetry points (Γ, J, K, J') along the surface Brillouin zone are labeled accordingly. Qualitatively, the results reported for the unpaired and paired DB wires, in the [110] and $[\bar{1}10]$ directions, are similar to those of Watanabe *et al.*[10] for unpaired DB wire in the $[\bar{1}10]$ direction and unpaired and paired DB wires in the $[\bar{1}10]$ and [110] directions. However, there are some differences in the shape of dispersion for the paired DB wire. Furthermore, since the calculations by Watanabe *et al.*[10] are done using density-functional theory, where band gaps are underestimated, quantitative comparison is not possible. For comparison with experiments, the only possibility is scanning tunneling spectroscopy (STS) based observations, which give information about the local density of states. In the context of this work, we cannot claim quantitative agreement with this setup because the observations get influenced by the applied tip voltage, Si band bending, and in some cases by the presence of other defects and dopants. Hitosugi *et al.*[11] have made these STS observations for a paired DB wire in the [110] direction and an unpaired DB wire in the $[\bar{1}10]$ direction. They compare their experimental results with the theoretical results of Watanabe *et al.*,[10] and they propose that their theoretically reported states agree with the experimentally observed features qualitatively. They find 0.5 eV band gap for the paired DB wire in the [110] direction. We find a band gap of about 0.75 eV. The difference could be due to the additional broadening introduced by the dephasing due to electron-phonon scattering[47] at the Si sur-

face. For an unpaired DB wire in the $[\bar{1}10]$ direction, they find a finite density of states at the Fermi energy, which is consistent with the near-midgap state found in our calculation. However, in order to make a quantitative comparison with the experimental STS results, we need to do a transport calculation including all the above-mentioned effects, which we postpone as future work. Qualitatively, our results show a similar trend as the experiments.

Figure 5 presents electronic band-structure calculation for DB clusters. The qualitative behavior can be attributed to a combined behavior of individual unpaired and paired DBs, which are 3.84 Å apart, with small shift due to bonding and/or broadening if the energies of different states are overlapping to start with. Figure 5(a) shows states due to a cluster of unpaired and paired DBs, 3.84 Å apart (model X). The resulting states consist of (1) a near-midgap dispersionless state about 0.44 eV above E_v (a shift of 20 meV as compared to isolated unpaired DB), (2) a π state about 70 meV below E_v (a shift of 10 meV as compared to isolated paired DB), and (3) a π^* state about 0.1 eV below E_c (a shift of 0.1 eV as compared to isolated paired DB). Since the π state is inside the valence band, it hybridizes with the valence-band states and thus has a small dispersion associated with it. However, the π^* state being inside the band gap is relatively isolated from the band states and hence is comparatively dispersionless.

Further, states due to a cluster of two paired DBs, 3.84 Å apart, (model XI) result in two π and two π^* states, as shown in Fig. 5(a). Since π states to start with are inside the valence band, they are already hybridized with the valence-band states. Therefore, the additional hybridization between these two π states results in very small additional dispersion. However, the case of two π^* states is very interesting. Since these two states are inside the band gap to start with, they hybridize with each other, giving rise to a bonding state about 0.16 eV below E_c and an antibonding state close to E_c.

Figure 5(b) shows the electronic structure calculation for a paired-unpaired-paired DBs cluster (model XII). The unpaired DB state stays the same as in Fig. 5(a), i.e., about 0.44 eV above E_v. However, due to two unpaired DBs, there are two π and two π^* states showing similar behavior as that of the two paired DBs cluster. However, one of the π^* states is slightly inside the conduction band, resulting in slight dispersion due to interaction with the conduction-band states. Figure 5(b) also shows the calculations for an unpaired-paired-unpaired DB cluster (model XIII). There are one π and one π^* state. The π state is similar to the one present in the unpaired-paired DBs cluster discussed in Fig. 5(a). However, the π^* state is very close to the conduction band and has a small dispersion as well, due to interaction with the conduction band. Additionally, there are two near-midgap states due to the unpaired DBs. These two DBs are 7.68 Å away and hence the resulting "bonding" and "antibonding" states slightly shift from the original energetic position of 0.44 eV above E_v. In Figs. 5(a) and 5(b), only the states inside or close to the band gap are shown. To the best of our knowledge, not much has been done theoretically for such DB clusters due to complexity of the calculations. Hersam *et al.*[29] have done STS measurements on such DB clusters. They find states inside the band gap, which are close to E_c, and states below E_v. We interpret that these states are due to paired DB clusters and find them consistent with our calculations. Since there are no midgap states in their experiment, we exclude the possibility of having unpaired DBs in this experiment.

V. CONCLUSIONS

We have reported the electronic band-structure calculations showing differences between states induced in Si band gap due to isolated DB, DB wires, and DB clusters. We show that the details of these states inside the band gap vary considerably from isolated DBs to DB wires to DB clusters. An unpaired DB behaves completely differently from a paired DB. Similarly, isolated DBs are different from DB wires and clusters. Furthermore, the dispersion in these states depends on the physical distance between the dangling bonds. Since these dangling bonds electronically interact over a characteristic length scale of 10 Å and the wave function decays exponentially with distance, the dispersion can be as large as 1 eV if DBs are 3.84 Å apart and can be as small as zero if the states are more than 20 Å apart. Thus, an isolated unpaired DB and a paired DB have dispersionless induced states. However, wires introduce a larger dispersion due to interactions amongst the DBs, resulting in hybridization. Similarly, for DB clusters, the states get slightly broadened if they are within the bands. Within the clusters, the states get shifted as a result of hybridization. Further, a good match with the experiments has been achieved.

ACKNOWLEDGMENTS

We thank G.-C. Liang and T. Raza for useful discussions. We acknowledge D. Kienle and K. H. Bevan for reviewing the paper. This work was supported by the NASA Institute for Nanoelectronics and Computing (INAC). Computational facilities were provided by the NSF Network for Computational Nanotechnology and nanoHUB.org.[48]

[1] J. Bardeen, Phys. Rev. **71**, 717 (1947).
[2] L. F. Wagner and W. E. Spicer, Phys. Rev. Lett. **28**, 1381 (1972).
[3] J. A. Stroscio, R. M. Feenstra, and A. P. Fein, Phys. Rev. Lett. **57**, 2579 (1986).
[4] R. J. Hamers, R. M. Tromp, and J. E. Demuth, Phys. Rev. B **34**, 5343 (1986).
[5] R. J. Hamers and J. E. Demuth, Phys. Rev. Lett. **60**, 2527 (1988).
[6] R. Wolkow and P. Avouris, Phys. Rev. Lett. **60**, 1049 (1988).
[7] R. A. Wolkow, Phys. Rev. Lett. **74**, 4448 (1995).
[8] H. N. Waltenburg and J. T. Yates, Jr., Chem. Rev. (Washington, D.C.) **95**, 1589 (1995).
[9] R. J. Hamers and Y. Wang, Chem. Rev. (Washington, D.C.) **96**,

1261 (1996).
[10] S. Watanabe, Y. A. Ono, T. Hashizume, and Y. Wada, Phys. Rev. B **54**, R17308 (1996).
[11] T. Hitosugi, T. Hashizume, S. Heike, Y. Wada, S. Watanabe, T. Hasegawa, and K. Kitazawa, Appl. Phys. A: Mater. Sci. Process. **66**, S695 (1998).
[12] D. A. Muller, T. Sorsch, S. Moccio, F. H. Baumann, K. Evans-Lutterodt, and G. Timp, Nature (London) **399**, 758 (1999).
[13] P. Zhang, E. Tevaarwerk, B.-N. Park, D. E. Savage, G. K. Celler, I. Knezevic, P. G. Evans, M. A. Eriksson, and M. G. Lagally, Nature (London) **439**, 703 (2006).
[14] H. Raza, K. H. Bevan, and D. Kienle, arXiv:cond-mat/0607226 (unpublished).
[15] M. McEllistrem, G. Haase, D. Chen, and R. J. Hamers, Phys. Rev. Lett. **70**, 2471 (1993).
[16] See, for example, S. Mahapatra, M. Alam, P. Bharath Kumar, T. R. Dalei, and S. Saha, Tech. Dig. - Int. Electron Devices Meet. **2004**, 105.
[17] N. Z. Butt, A. Chang, R. Bashir, H. Raza, J. Liu, and D.-L. Kwong, Appl. Phys. Lett. **88**, 112901 (2006).
[18] G. P. Lopinski, D. D. M. Wayner, and R. A. Wolkow, Nature (London) **406**, 48 (2000).
[19] T.-C. Shen, C. Wang, G. C. Abeln, J. R. Tucker, J. W. Lyding, Ph. Avouris, and R. E. Walkup, Science **268**, 1590 (1995).
[20] K. Stokbro, C. Thirstrup, M. Sakurai, U. Quaade, Ben Yu-Kuang Hu, F. Perez-Murano, and F. Grey, Phys. Rev. Lett. **80**, 2618 (1998).
[21] Z. Liu, L. C. Feldman, N. H. Tolk, Z. Zhang, and P. I. Cohen, Science **312**, 1024 (2006).
[22] P. G. Piva, G. A. DiLabio, J. L. Pitters, J. Zikovsky, M. Rezeq, S. Dogel, W. A. Hofer, and R. A. Wolkow, Nature (London) **435**, 658 (2005).
[23] M. McEllistrem, M. Allgeier, and J. J. Boland, Science **279**, 545 (1998).
[24] T. Hitosugi, S. Heike, T. Onogi, T. Hashizume, S. Watanabe, Z.-Q. Li, K. Ohno, Y. Kawazoe, T. Hasegawa, and K. Kitazawa, Phys. Rev. Lett. **82**, 4034 (1999).
[25] D. J. Lepoine, Phys. Rev. B **6**, 436 (1972).
[26] E. Artacho and Felix Yndurain, Phys. Rev. Lett. **62**, 2491 (1989).
[27] M. Xiao, I. Martin, E. Yablonovitch, and H. W. Jiang, Nature (London) **430**, 435 (2004).
[28] M. C. Hersam, N. P. Guisinger, J. Lee, K. Cheng, and J. W. Lyding, Appl. Phys. Lett. **80**, 201 (2002).
[29] M. C. Hersam, N. P. Guisinger, and J. W. Lyding, Nanotechnology **11**, 70 (2000).
[30] M. Cakmak and G. P. Srivastava, Surf. Sci. **532**, 556 (2003).
[31] G. P. Srivastava, *Theoretical Modelling of Semiconductor Surfaces* (World Scientific, River Edge, NJ, 1999).
[32] J. Cerda and F. Soria, Phys. Rev. B **61**, 7965 (2000).
[33] D. Kienle, K. H. Bevan, G.-C. Liang, L. Siddiqui, J. I. Cerda, and A. W. Ghosh, J. Appl. Phys. **100**, 043715 (2006).
[34] G.-C. Liang and A. W. Ghosh, Phys. Rev. Lett. **95**, 076403 (2005).
[35] M. S. Hybertsen and S. G. Louie, Phys. Rev. Lett. **55**, 1418 (1985).
[36] M. Rohlfing, P. Krüger, and J. Pollmann, Phys. Rev. B **48**, 17791 (1993).
[37] T. Rakshit, G.-C. Liang, A. W. Ghosh, and S. Datta, Nano Lett. **4**, 22 (2004).
[38] A. Ramstad, G. Brocks, and P. J. Kelly, Phys. Rev. B **51**, 14504 (1995).
[39] M. J. Frisch, G. W. Trucks, H. B. Schlegel, G. E. Scuseria, M. A. Robb, J. R. Cheeseman, J. A. Montgomery, Jr., T. Vreven, K. N. Kudin, J. C. Burant, J. M. Millam, S. S. Iyengar, J. Tomasi, V. Barone, B. Mennucci, M. Cossi, G. Scalmani, N. Rega, G. A. Petersson, H. Nakatsuji, M. Hada, M. Ehara, K. Toyota, R. Fukuda, J. Hasegawa, M. Ishida, T. Nakajima, Y. Honda, O. Kitao, H. Nakai, M. Klene, X. Li, J. E. Knox, H. P. Hratchian, J. B. Cross, C. Adamo, J. Jaramillo, R. Gomperts, R. E. Stratmann, O. Yazyev, A. J. Austin, R. Cammi, C. Pomelli, J. W. Ochterski, P. Y. Ayala, K. Morokuma, G. A. Voth, P. Salvador, J. J. Dannenberg, V. G. Zakrzewski, S. Dapprich, A. D. Daniels, M. C. Strain, O. Farkas, D. K. Malick, A. D. Rabuck, K. Raghavachari, J. B. Foresman, J. V. Ortiz, Q. Cui, A. G. Baboul, S. Clifford, J. Cioslowski, B. B. Stefanov, G. Liu, A. Liashenko, P. Piskorz, I. Komaromi, R. L. Martin, D. J. Fox, T. Keith, M. A. Al-Laham, C. Y. Peng, A. Nanayakkara, M. Challacombe, P. M. W. Gill, B. Johnson, W. Chen, M. W. Wong, C. Gonzalez, and J. A. Pople, GAUSSIAN 03, Revision B.03, Gaussian, Inc., Wallingford, CT, 2004.
[40] Atomic coordinates for Si(001)-(2×1)-AD unit cell: (Si, 1.162 00, 0.000 00, −0.921 00); (Si, 3.305 59, 0.000 00, −0.213 00); (Si, 0.066 00, 1.919 79, −1.498 50); (Si, 3.740 59, 1.919 79, −1.469 50); (Si, 1.950 79, 1.919 79, −2.955 00); (Si, 5.734 38, 1.919 79, −2.718 00); (Si, 1.906 79, 0.000 00, −4.227 50); (Si, 5.754 38, 0.000 00, −4.070 50). The remaining 24 Si and four H atoms have the same coordinates as those of the last 24 Si and four H atoms of the H:Si(001)-(2×1) unit cell (Ref. 41).
[41] Atomic coordinates for H:Si(001)-(2×1) unit cell: (H, 0.311 40, −0.070 20, 0.858 90); (H, 3.528 20, −0.070 20, 0.858 90); (Si, 0.805 00, 0.000 00, −0.524 00); (Si, 3.034 59, 0.000 00, −0.524 00); (Si, 0.075 00, 1.919 79, −1.498 50); (Si, 3.764 59, 1.919 79, −1.498 50); (Si, 1.919 79, 1.919 79, −2.931 00); (Si, 5.759 38, 1.919 79, −2.710 00); (Si, 1.919 79, 0.000 00, −4.211 50); (Si, 5.759 38, 0.000 00, −4.070 50); (Si, 0.000 00, 0.000 00, −5.430 00); (Si, 3.839 59, 0.000 00, −5.430 00); (Si, 0.000 00, 1.919 79, −6.787 50); (Si, 3.839 59, 1.919 79, −6.787 50); (Si, 1.919 79, 1.919 79, −8.145 00); (Si, 5.759 38, 1.919 79, −8.145 00); (Si, 1.919 79, 0.000 00, −9.502 50); (Si, 5.759 38, 0.000 00, −9.502 50); (Si, 0.000 00, 0.000 00, −10.864 00); (Si, 3.839 59, 0.000 00, −10.864 00); (Si, 0.000 00, 1.919 79, −12.221 50); (Si, 3.839 59, 1.919 79, −12.221 50); (Si, 1.919 79, 1.919 79, −13.579 00); (Si, 5.759 38, 1.919 79, −13.579 00); (Si, 1.919 79, 0.000 00, −14.936 50); (Si, 5.759 38, 0.000 00, −14.936 50); (Si, 0.000 00, 0.000 00, −16.294 00); (Si, 3.839 59, 0.000 00, −16.294 00); (Si, 0.000 00, 1.919 79, −17.651 50); (Si, 3.839 59, 1.919 79, −17.651 50); (Si, 1.919 79, 1.919 79, −19.009 00); (Si, 5.759 38, 1.919 79, −19.009 00); (Si, 1.919 79, 0.000 00, −20.366 50); (Si, 5.759 38, 0.000 00, −20.366 50); (H, 0.719 59, 0.000 00, −21.215 20); (H, 3.119 99, 0.000 00, −21.215 20); (H, 4.559 18, 0.000 00, −21.215 20); (H, 6.959 58, 0.000 00, −21.215 20). The unit cells for Figs. 1(b) and 1(d) can be generated by removing respective H atom(s).
[42] T. Blomquist and G. Kirczenow, Nano Lett. **6**, 61 (2006).
[43] R. Dennington II, T. Keith, J. Millam, K. Eppinnett, W. L. Hovell, and R. Gilliland, GAUSSVIEW, Version 3.0, Semichem, Inc., Shawnee Mission, KS, 2003.
[44] R. I. G. Uhrberg, G. V. Hansson, J. M. Nicholls, and S. A. Flodström, Phys. Rev. B **24**, 4684 (1981).

[45] L. S. O. Johansson, R. I. G. Uhrberg, P. Martensson, and G. V. Hansson, Phys. Rev. B **42**, 1305 (1990).
[46] R. F. Pierret, *Advanced Semiconductor Fundamentals* (Addison-Wesley, Reading, MA, 1989), Sec. 504.
[47] H. Raza, arXiv:cond-mat/0703236 (unpublished).
[48] nanoHUB.org is a web site dedicated to advancing nanotechnology through theory, modeling, and simulation for research and education.